

Oxygen Phonon Branches in $\text{YBa}_2\text{Cu}_3\text{O}_{7-x}$

L. Pintschovius, D. Reznik*, W. Reichardt

Forschungszentrum Karlsruhe, Institut für Festkörperphysik, P.O.B. 3640, D-76021 Karlsruhe, Germany

Y. Endoh, H. Hiraka

Institute for Material Research, Tohoku University, Katahira, Aoba-ku, Sendai, 980-8577, Japan

J.M. Tranquada

Physics Department, Brookhaven National Laboratory, Upton, NY 11973, USA

H. Uchiyama, T. Masui, S. Tajima

Superconductivity Research Laboratory, ISTEC, Shinonome, Koutu-ku, Tokyo, 135-0062, Japan

(Dated: March 22, 2024)

We report results of inelastic neutron scattering measurements of phonon dispersions in optimally doped $\text{YBa}_2\text{Cu}_3\text{O}_{6.95}$ and compare them with model calculations. The focus is on the in-plane oxygen bond-stretching phonon branches. The study of these modes is complicated by anticrossings with c-axis-polarized branches; such effects are interpreted through lattice-dynamical shell-model calculations. The in-plane anisotropy of the bond-stretching phonons was firmly ascertained from measurements on a detwinned sample. Studying not only the in-plane modes involving in-phase motion for the two Cu-O layers within a unit cell but also those with opposite-phase motion was of great help for establishing a clear experimental picture. The measurements confirm that the in-plane oxygen bond-stretching phonon branches disperse steeply downwards from the zone center in both the a and the b directions indicating a strong electron-phonon coupling. For the b-axis-polarized bond-stretching phonons, there is an additional feature of considerable interest: a sharp local frequency minimum was found to develop on cooling from room temperature to $T = 10$ K at wave vector $q = 0.27$ r.l.u..

PACS numbers: 74.25.Kc, 63.20.Kr, 74.72.Bk

I. INTRODUCTION

Numerous inelastic neutron scattering investigations[1, 2, 3] on high- T_c superconductors and their insulating parent compounds have shown that the high-energy Cu-O bond-stretching modes soften considerably on doping. It was advocated from the very beginning[4] that this phonon softening indicates a strong electron-phonon coupling, but it attracted nevertheless only limited attention because phonons were widely considered to be irrelevant for the mechanism of high- T_c superconductivity. Recently, renewed interest in the phonons came from observations made by angular resolved photoemission spectroscopy of an abrupt change of electron velocity at 50-80 meV which was interpreted as evidence for an ubiquitous strong electron-phonon coupling in high- T_c superconductors[5, 6]. Further interest was generated by theories[7, 8, 9] predicting an inhomogeneous charge distribution in the Cu-O planes, in particular in the form of stripes. In superconducting samples, charge stripes are assumed to be dynamic in nature which makes it very difficult to detect them. They might reveal themselves by coupling to the phonons[10, 11, 12] thus making inelastic neutron scattering an appealing technique. Naively, one might expect precursor phenomena to charge-density-wave (CDW) formation similar to what has been observed in one-dimensional conductors such as KCP some time ago[13]. There, a dip develops in the phonon dis-

persion of the longitudinal acoustic branch in a narrow range of momentum transfer about a wavevector related to the spanning vector $2k_F$ of the Fermi surface.

In the cuprates, the most pronounced effects are expected for the Cu-O bond stretching vibrations because the Cu-O bond length will be significantly modulated by the extra charge residing on the stripes. Early investigations[14] of the phonons in $\text{YBa}_2\text{Cu}_3\text{O}_{7-x}$ have indeed shown that the O bond-stretching vibrations within the Cu-O planes behave in a normal way in insulating samples but in an apparently anomalous way in optimally doped ones: the frequency of these phonons decreases abruptly when going from the zone center along the $[100]$ ($=a^*$) direction or the $[010]$ ($=b^*$) direction about halfway to the zone boundary. In addition, the phonon peaks become very poorly defined in this q -range. Unfortunately, twinning of the samples did not allow one to decide whether the phonons in question really acquire a very large intrinsic linewidth or whether the observed peaks are so broad simply because the superimposed contributions from the a^* and the b^* directions differ in energy. A recent inelastic neutron scattering investigation [15] using pulsed neutrons came to the conclusion that the Cu-O bond-stretching branch along the b^* direction has a steep, but continuous downward dispersion whereas the branch along a^* splits into two in the middle of the zone. The latter finding was tentatively interpreted as a signature of charge stripes. We will discuss this interpre-

tation in the light of our own results.

The present paper describes results of inelastic neutron scattering measurements made by the triple-axis technique on detwinned as well as on twinned samples of optimally doped $\text{YBa}_2\text{Cu}_3\text{O}_{6.95}$ aiming at elucidating the anomalous behavior of the bond-stretching modes. The measurements on the detwinned samples were key to achieving a better understanding of the a-b anisotropy and of the seemingly anomalous lineshapes. We show that very complex intensity distributions can be explained as resulting from an interaction of phonon branches having the same symmetry but a different polarization [16]. The line broadenings due to anti-crossings partly mask a more important reason for anomalous lineshapes, i.e. a sharp drop of phonon frequencies within a narrow range of wave vectors along b^* observed at low temperatures. As has been pointed out in a separate publication [17] this peculiar behavior is observed only at low temperatures and strongly suggests dynamic charge stripe formation with a period of about four lattice constants.

The rest of the paper is organized as follows. Experimental details are given in the following section. The model used to simulate the phonon dispersions and scattering intensities is described in Sec. III. These calculations are essential for making sense of the measurements, which are presented in Sec. IV. A discussion of the results and conclusions are given in Sec. V and VI, respectively. Appendix A provides a brief description of anti-crossing behavior between neighboring phonon branches. The special force constants, beyond the shell model, required to simulate the observations are described in Appendix B.

II. EXPERIMENTAL

The first series of measurements was performed on a detwinned sample. It consisted of 26 detwinned single crystals co-aligned with an effective mosaic spread of ~ 3 degrees. The total volume of the sample was $\sim 1 \text{ cm}^3$. Unfortunately, the crystals cleaved into many small pieces after the first cooling cycle, and therefore additional measurements had to be performed on twinned samples. The next round of measurements was carried out on a composite sample weighing a total of 31 g which was used previously for a part of the pulsed neutron measurements of Chung et al [15]. However, this sample was not very well suited for triple-axis measurements because the lateral dimensions were too large compared to the size of the neutron beam. Moreover, high-precision measurements of the c-axis lattice constant of the individual crystals revealed that some of them were underdoped. Based on these findings, another composite sample was assembled out of 3 optimally doped ($\text{YBa}_2\text{Cu}_3\text{O}_{6.95}$, $T_c = 93 \text{ K}$) single crystals of combined volume of $\sim 1.5 \text{ cm}^3$ co-aligned with a mosaic spread of 2.2 degrees. All the temperature dependent studies were done on this sample.

The experiments were carried out on the triple-axis spectrometer IT located at the ORPHEE reactor using doubly focusing monochromator (Cu111 or Cu220) and analyzer (PG 002) crystals. Specifically, Cu111 was used as monochromator for the measurements on the detwinned sample to maximize the intensity whereas Cu220 was used for the measurements on the twinned samples to achieve high resolution. The energy resolution at energy transfer of $E \sim 70 \text{ meV}$ was $\Delta E = 4.6 (2.9) \text{ meV}$ (FWHM) for the Cu111 (Cu220) monochromator and a final energy $E_f = 14.7 \text{ meV}$. The measurements were carried out in different scattering planes in order to elucidate the eigenvectors of the atomic vibrations in question. Most measurements were performed at $T = 12 \text{ K}$ but selected phonons were also studied at higher temperatures up to $T = 300 \text{ K}$.

III. PHONON MODEL CALCULATIONS

In measurements on compounds with many atoms in the unit cell, an assignment of phonon peaks to particular modes has to be based on model calculations. For this purpose, extensive model calculations were carried out prior to and in parallel with the experiments. The model used as a starting point was the common interaction potential model reported in Ref. 19, which is quite successful in describing the phonon dispersion curves of a number of cuprates. In the framework of this model, $\text{YBa}_2\text{Cu}_3\text{O}_7$ is considered as an ionic compound, and the interatomic interactions are modeled as a sum of Coulomb forces and short range repulsive forces. In addition, the polarizability of the atoms is taken into account using the shell model formalism. For a metallic compound like $\text{YBa}_2\text{Cu}_3\text{O}_7$ a term accounting for screening by free carriers is added. This model gives a decent description of most of the available data shown in Ref. 1. We further improved upon the agreement between model and experiment by tuning the parameters; the refined parameters are listed in Table I. However, it was already clear before the present study that extra ad hoc interactions are required to adequately describe the oxygen bond-stretching modes.

Experiments [1, 14] have shown that the bond-stretching phonon frequencies are strongly renormalized. This effect is much stronger in the [100] and in the [010] directions than in the [110] direction. It leads to a downward dispersion from zone center to zone boundary [14] which cannot be reproduced by simply tuning the parameters of the common interaction potential model [18]. Adding to the model a negative breathing deformability lowers the calculated energy of the planar breathing mode, which is the endpoint of the bond-stretching phonon branch in the [110] direction. At the same time, this term lowers the energy of the corresponding branches in the [100] and the [010] directions, but by only half the amount of that in the [110] direction. Therefore, additional terms were added lowering specifically the energies

of the "halfbreathing" modes at the zone boundary of the $[100]$ and $-$ with a different parameter $-$ of the $[010]$ direction. The extra terms are described in detail in Appendix B.

To proceed further with this discussion, it is necessary to illustrate the situation with actual data. Figure 1 compares calculated dispersions with measured O bond-stretching modes dispersing along $[010]$ and involving opposite-phase motion for the two $Cu-O$ layers within a unit cell ($\frac{1}{2}$ symmetry). The fit to the 200-K data with the additional terms discussed above is indicated by the magenta curve. This fit matches the data well at the zone center and boundary, but falls significantly above the data in the middle of the zone. To remedy this deficiency, a further term was included that produces a maximum effect at the halfway point but zero effect both at the zone center and at the zone boundary. The resulting fit is indicated by the red line in Fig. 1. An important result of the present investigation is the observation of an anomalous softening in the $[010]$ direction within a rather narrow range of wave vectors on cooling from room temperature to low temperatures. In order to fit the 10 K data, an additional term producing a sharper effect halfway to the zone boundary had to be included with the resulting fit indicated by the blue line in Fig. 1. We believe that all of the extra terms we have added reflect the electron-phonon coupling resulting from doping holes into the CuO_2 planes.

Before continuing on, it may be useful to make contact with recent theoretical work. Bohnen, Heid, and Krauss [23] have calculated the phonon dispersions for $YBa_2Cu_3O_7$ using a method based on evaluating the band structure in the local-density approximation (LDA). Their results successfully match the experimental $\frac{1}{2}$ branch at 200 K (see Ref. [17]) though they do not predict the temperature induced softening halfway to the zone boundary. Further, their calculations reproduce the corresponding $\frac{1}{2}$ branch along $[100]$ very well (Fig. 8). The LDA results provide some justification for the ad hoc interactions that have been discussed above and point at the unconventional nature of the temperature dependence observed in the $[010]$ direction.

We note again that Fig. 1, which illustrates the effects of the special terms, was prepared for branches of $\frac{1}{2}$ -symmetry. Phonons of $\frac{1}{2}$ -symmetry are distinguished from those of $\frac{1}{2}$ -symmetry in that the atoms in the $Cu-O$ bi-layer move in opposite phase instead of in-phase. For modes of $\frac{1}{2}$ -symmetry, the downward dispersion of the bond-stretching mode leads to anti-crossings with branches of the same symmetry which originally have a different polarization but that hybridize with the bond-stretching phonons where they are close in energy (readers who are not familiar with such effects are referred to APPENDIX A). The anti-crossings are naturally explained by the model, and the model calculations for $\frac{1}{2}$ frequencies and intensities agree well with the experimental measurements, as will be shown in the next section. It happens that the branches of $\frac{1}{2}$ -symmetry are much

less affected by anti-crossing effects.

IV. RESULTS AND ANALYSIS

A. Low temperature measurements

Experimental spectra obtained on the detwinned sample are plotted in Figs. 2,3. The two series of scans were conducted along lines from the $(4,1,0)$ reciprocal lattice point to $(3.5,1,0)$ and from $(1,4,0)$ to $(1.35,0)$, respectively. These lines were chosen because (i) the inelastic structure factors of the bond-stretching modes are quite favorable here and (ii) these choices allowed us to exploit focusing effects. The figures further show simulated spectra calculated with the help of the lattice dynamical model described in the previous section. We note that the full resolution in q and w was taken into account for the simulations. There is obviously very good agreement between the experimental and the calculated spectra. Another way to visualize this agreement is to represent both types of spectra as (color coded) contour plots (Figs. 4,5). The plots computed from the simulated spectra also show the phonon dispersion curves calculated from the same model for the high symmetry directions. All the depicted branches are of the same symmetry, i.e. $\frac{1}{2}$ (Figs. 2,4) and $\frac{1}{2}$ (Figs. 3,5), respectively (in order to distinguish phonon branches along a^* from those along b^* we add a prime to the symmetry labels for the b -axis branches). They are sometimes simply labelled as longitudinal optic branches. However, this labelling is rather imprecise as there are other phonon branches with a different symmetry having a longitudinal character as well. On the other hand, the polarization may be very different for different branches of the same symmetry class: as will be discussed below, some of the $\frac{1}{2}(\frac{1}{2})$ branches are c -axis polarized and hence are not observable for momentum transfers within the $[100]$ - $[010]$ -scattering plane. Nevertheless, they cannot be ignored in the interpretation of our data because they hybridize with in-plane polarized branches in certain parts of the Brillouin zone (because they belong to the same symmetry class) and hence show up in the scans under discussion.

Our conclusions regarding c -axis-polarized $\frac{1}{2}$ branches are based on previous studies. In particular, the c -axis polarized branches with zone-center energies of 62 meV and 54 meV, respectively, were studied in Ref. 14, where they were measured with a large c^* -component of the momentum transfer. A summary of the available data from the present and from previous studies [1] together with the calculated dispersion curves in the whole range of phonon energies is shown in Fig. 6.

As already indicated in Sec. II, a very important step in establishing the dispersions of the bond-stretching modes has come from studies of branches with $\frac{1}{2}$ -symmetry, i.e. the modes where the atoms in the $Cu-O$ bi-layer move in opposite phase. We found that the

bond-stretching vibrations of ϵ_1 -symmetry and those of ϵ_4 -symmetry have very similar energies, as one should expect from the weak coupling across the Y atom. What makes a study of the ϵ_4 -bond-stretching branches very attractive is the fact that mixing with c-axis polarized modes is less of a problem. The ϵ_4 -modes had to be studied on a twinned sample. The measurements were made around the (3,0,2) reciprocal lattice point. Representative spectra are shown in Fig. 7; see Ref. 17 for further data. As one can see, high resolution allowed us to separate the modes for the a^* direction and for the b^* direction, respectively. The results for the a^* direction are summarized in Fig. 8. The results for the b^* direction are included in Fig. 1.

The good agreement between our model and the experimental gives support to a rather conventional picture of phonon dispersion with a notable exception of anomalous dispersion of plane oxygen bond-stretching vibrations calling for the special terms. The following picture emerges from our analysis: the branches starting at $E = 67$ meV and 73 meV, respectively, have in-plane Cu-O bond-stretching character with the atoms in the Cu-O bilayer moving in-phase. The energy difference at the zone center can be explained entirely by the difference in the Cu-O bond lengths along a and b . Both branches show a steep downward dispersion halfway to the zone boundary. The b -polarized branch even has a pronounced local minimum at $q = 0.27$ r.l.u. whereas the a -polarized branch does not have such a local minimum but is quite flat for $q > 0.3$ r.l.u. As will be discussed in a later section, the local frequency minimum in the b -polarized branch is seen only at low temperatures. The dispersion of the bond-stretching modes with ϵ_1 -symmetry is, however, somewhat obscured by an anticrossing with a c-axis polarized branch which starts from the Ag mode at 62 meV. In the b^* direction, a further complication arises from the presence of another branch of the same symmetry in the energy region of interest: the corresponding zone-center mode has an energy of $E = 59$ meV and involves longitudinal Cu-O chain bond-stretching vibrations. When approaching the zone boundary, there is another problem for the determination of the bond-stretching phonon frequencies: the intensities associated with bond-stretching modes overlap with those from other branches dispersing upwards in the energy range 45-55 meV (Figs. 4,5). They have, in principle, in-plane oxygen bond-bending character, but there will be inevitably some hybridization with the bond-stretching mode once the two modes are very close in energy. We note that this hybridization vanishes only close to the zone boundary, because there the bond-bending modes and the bond-stretching modes belong to different symmetry classes.

Motivated by reports [15] of an unusual dispersion of transverse bond-stretching branches in $\text{YBa}_2\text{Cu}_3\text{O}_{7-x}$ we studied these branches as well. As can be seen in Fig. 9, our data do not support the claim that the transverse branch along b^* has a rather strong dispersion up to $q = 0.25$; to the contrary, this branch has as little disper-

sion as the corresponding one along a^* [20]. Figure 9 also shows the TO branch starting from the longitudinal chain O mode. There was no problem to follow this branch up to the zone boundary but attempts to follow the corresponding branch in the longitudinal direction had only very limited success. We learned from our model calculations that the LO branch starting from the chain O mode hybridizes very strongly with the other branches of the same symmetry – in particular, with the c polarized apical O vibrations – already at small wave vectors. For this reason, we were unable to follow this branch beyond $q = 0.15$ r.l.u.

B. Temperature dependence

Selected phonons were studied as a function of temperature on a twinned sample. We found that the frequencies of the zone center phonons and of the zone boundary phonons show very little change when going from $T = 12$ K to room temperature (Fig. 10). A certain increase in linewidth as is evident for the zone boundary phonon is typical of anharmonic behavior. The decrease of the phonon intensities with increasing temperature can be accounted for by the Debye-Waller-factor. Our finding that even the strongly renormalized zone boundary phonons show very little temperature dependence was in conflict with claims made by Chung et al. [15] that the bond-stretching phonons show an anomalous temperature behavior throughout the Brillouin zone (see Fig. 9 of Ref. 15). Therefore, we finally embarked on a detailed study to check these claims. Although we could not confirm many of the temperature induced changes reported in Ref. 15 we found indeed a very pronounced effect of certain phonon modes. As explained in a separate publication [17] a downward shift of spectral weight by at least 10 meV was observed for b polarized bond-stretching phonons of ϵ_4' -symmetry at $q = 0.27$ r.l.u. on cooling from room temperature to $T = 12$ K. The temperature evolution starts well above the superconducting transition temperature, i.e. at about $T = 200$ K. Data for $T = 200$ K have been included in Fig. 1. These data were important for adjusting the parameters of our model. When the parameters were adjusted to better fit the data of the ϵ_4' -branches, we obtained an improved fit for the ϵ_1 -branches as well, which further validates our analysis.

V. DISCUSSION

The present results qualitatively confirm the results of an early study by Reichardt [14] but also go much beyond it in that we were able to elucidate the a - b anisotropy of the bond-stretching modes. Furthermore, we have gained some insight into the origin of the broad intensity distributions observed in the region halfway to the zone boundary. It appears that the complex line-

shapes observed for a-polarized bond-stretching modes of Γ_1 -symmetry can be attributed in large part to anticrossings with other branches of the same symmetry. We agree with the observation reported in Ref. 15 that the bond-stretching branch along a^* splits into two branches halfway to the zone boundary; however, we disagree on the interpretation. The phenomenon is the natural consequence of hybridization between the O in-plane bond-stretching modes and those of apical O vibrations along c . This phenomenon is illustrated in Fig. 11 for the zone boundary point. As for the b direction, there are two reasons for the observed complex line shapes: (i) anticrossings of different branches and (ii) the anomalously steep dispersion—probably associated with very broad intrinsic linewidths—at q halfway to the zone boundary. In order to study the importance of (ii) we simulated the scans shown in Figs. 3,5 using the model fitted to the 200 K data, i.e. a model giving a smooth dispersion throughout the Brillouin zone. The following conclusions are drawn from this simulation (Fig. 12). Although the differences between Fig. 12 and Fig. 5b are somewhat subtle, there is definitely a better agreement between the experimental results displayed in Fig. 5a and the calculated ones in Fig. 5b than with those in Fig. 12. This indicates that the bond-stretching branch of Γ_1 -symmetry exhibits the same type of anomalous low- T behaviour as its counterpart of Γ_4' -symmetry. This conclusion is in line with evidence for an anomalous temperature dependence of Γ_1 -modes reported in Ref. 15. On the other hand, it would have been extremely difficult to establish details of the temperature dependence from measurements of the Γ_1 -branches alone in view of the formidable complication due to the anticrossings. Twinning of the sample further aggravates the situation considerably. Therefore, it is not surprising that the temperature dependence reported in Ref. 15 agrees with our results only on a qualitative level.

Measurements of the O in-plane bond-stretching phonons in optimally doped $\text{La}_{1.85}\text{Sr}_{0.15}\text{CuO}_4$ revealed a considerable broadening of the phonon lines for $q > 0.1 \text{ r.l.u.}$ [1, 2]. This broadening was found to be particularly pronounced around $q = (0.3, 0, 0)$ [2]. We expect a similar effect for optimally doped YBCO. Unfortunately, the problems for extracting linewidths discussed above do not allow us to deduce intrinsic phonon linewidths from the available data. We hope to achieve progress on this matter by a study of the Γ_4 resp. the Γ_4' modes on a detwinned sample.

Our model calculations indicate that the observed a - b anisotropy of the bond-stretching branches can be largely attributed to the orthorhombicity of the structure (apart from the anomalous temperature dependence along b^*) [22]. That is to say, the general energy difference between the two directions is reproduced by a simple potential model in conjunction with the experimental difference between the a and b lattice parameters. Further, the special terms needed to lower the zone boundary frequencies are of similar size. This contrasts with the re-

sults of a previous study of underdoped $\text{YBa}_2\text{Cu}_3\text{O}_{6.6}$ which had shown a much stronger a - b anisotropy at the zone boundary [27] which remains to be understood.

We have already mentioned in Sec. III the results of a recent *ab-initio* calculation [23] of the phonon dispersion in $\text{YBa}_2\text{Cu}_3\text{O}_7$ using Density Functional Theory in the local density approximation. The theory quantitatively predicts the frequency drop from the zone center to the zone boundary for the bond-stretching modes both along a^* and b^* at $T = 200 \text{ K}$; however, it also predicts a considerable downward dispersion for the $[110]$ direction as well ($\sim 8 \text{ meV}$) which is not borne out by experiment [14]. (Also, it is not possible to check the doping dependence because of the known limitations of LDA for describing the correlated-insulator parent compound, $\text{YBa}_2\text{Cu}_3\text{O}_6$.) Turning to a different mode, the theory makes an accurate prediction of a rather low frequency for the longitudinal chain O vibrations (61.5 meV). This is not quite as low as observed in experiment [28] (59 meV) but much lower than expected from the simple potential model [18] (75 meV) in which the Cu-O potential was assumed to be the same for the Cu-O chains and for the Cu-O planes. Unfortunately, we were unable to check the theoretical predictions that the longitudinal branch starting from the chain O mode has a strong downward dispersion and exhibits a local minimum at about halfway to the zone boundary, related to Fermi surface nesting of chain O electronic states. The strong mixing of the chain O mode with other modes of the same symmetry did not allow us to isolate the contributions of the chain O vibrations from the rest.

We note that in another cuprate, i.e. $(\text{La,Sr})_2\text{CuO}_4$, the phonon renormalization upon doping is also much stronger in the $[100]$ direction than in the $[110]$ direction [1]. Thus, this behavior seems to be common to Cu-O planes, but independent of extraneous features such as chains. The doping dependence and spatial anisotropy of the phonon softening appear to be captured by a calculation in which the t - J model is extended to explicitly include electron-phonon couplings. [24, 25]. Rosch and Gunnarsson [24] have evaluated the doping and q dependence of the O bond-stretching mode of a Cu-O layer through a t - J model with electron-phonon interactions derived from a three-band model. With their purely two-dimensional model, they obtain the correct anisotropy between the $[1,1]$ and $[1,0]$ directions, and reasonable results for the doping- and q -dependent softening of the mode along the $[1,0]$ direction.

From the discussion above, it is evident that the lattice dynamics of $\text{YBa}_2\text{Cu}_3\text{O}_7$ is less anomalous than advocated in Ref. 15, but nevertheless we think that the behavior of the bond-stretching modes indicates a strong electron-phonon coupling. The question of whether or not this electron-phonon coupling is relevant for high T_c superconductivity cannot be directly answered from the phonon data alone. From their theoretical analysis, Bohnen, Heid, and Krase [23] came to the conclusion that conventional electron-phonon coupling is much too

weak to explain a high T_c , in contrast to the case of MgB_2 where conventional electron-phonon does seem to explain the observed T_c [29].

V I. C O N C L U S I O N S

The present study has elucidated the a-b anisotropy of the plane-polarized bond-stretching vibrations in optimally doped $YBa_2Cu_3O_{6.95}$. We concluded that the bond-stretching branches show a steep downward dispersion in both the a and the b directions at $q = 0.25$ r.l.u. that leads to anti-crossings with c polarized branches. The resulting anti-crossing gaps can be explained by lattice dynamical calculations using a shell model. In the a direction, the bond-stretching mode of Γ_1 -symmetry is strongly hybridized with a c-polarized branch over a large part of the Brillouin zone, which explains the "splitting" of this branch reported in Ref. 15 in a natural way. The dispersion of the bond-stretching branches is very well reproduced by density-functional theory [23] if the comparison is based on 200 K data, whereas the pronounced softening observed in b-polarized branches at low T remains unexplained. Although the pronounced renormalization of zone boundary bond-stretching modes on going from insulating 0.6 to superconducting 0.7 indicates a strong electron-phonon coupling, theory [23] suggests that it is too weak to be relevant for high T_c superconductivity. Thus, the temperature effect, presented in detail in Ref. 17, seems to be the most anomalous phenomenon in the phonon properties of optimally doped YBCO.

A c k n o w l e d g m e n t s

We are indebted to Dr. Y. Shiohara and to Dr. S. Koyama at Superconductivity Research Laboratory for their help in growing the YBCO crystals. This work was partially supported by the New Energy and Industrial Technology Development Organization (NEDO) as Collaborative Research and Development of Fundamental Technologies for Superconductivity Applications. JMT is supported by the U.S. Department of Energy's Office of Science under Contract No. DE-AC02-98CH10886. This work was partially supported by the Japan Science and Technology Agency within the CREST project. This project has been also supported by the Grant in Aid for Scientific Research from the Japan Society of Promotion of Science.

A P P E N D I X A : A P P E N D I X A : A N T I - C R O S S I N G B E H A V I O R

$YBa_2Cu_3O_7$ has 13 atoms in the unit cell and hence there are 39 branches of the phonon dispersion in each direction. These branches can be grouped according

to symmetry of the eigenvectors of the atomic displacements. For the case of the [100] or the [010] direction, there are four different symmetry classes. Within each subset of dispersion curves, the polarization may be very different. Still, none of the branches is allowed to cross another one of the same subset. If, as a result of the special nature of the interatomic interactions, two branches tend to cross each other in a particular part of the Brillouin zone, this will lead to a mixing of the polarization patterns and to a mutual repulsion of the eigenfrequencies (exactly as in the problem of coupled harmonic oscillators). However, the degree of hybridization and the strength of the repulsion cannot be predicted from general principles but depend on the symmetry of the crystal lattice and the peculiarities of the interatomic interactions. For illustrative purposes, we consider the following case: a simple interatomic potential model [18] predicts a flat dispersion for the two topmost branches of Γ_1 -symmetry in the a direction (Fig. 13). These two branches have in-plane polarization and c-axis polarization, respectively. As a consequence, the inelastic scattering structure factors calculated for momentum transfers along the line $(3+\pi, 0, 0)$, i.e. in the basal plane, will be very different for the two branches. In a corresponding neutron scattering experiment, only the upper branch will be detected. The situation dealt with so far corresponds to the situation found in 0.6. In 0.7, however, the upper branch acquires strong dispersion from electron-phonon coupling effects as discussed in this paper. For the sake of simplicity, we have simulated such effects by adding a single special term to the dynamical matrix lowering the frequency of only the bond-stretching vibrations. The term is designed to produce a maximum effect at $q = 0.25$ r.l.u. (for details, see APPENDIX B). This term was tuned to reduce the frequency of the bond-stretching vibrations at $q = 0.25$ to below that of the apical O vibrations. As a consequence, phonons of the lower branch acquire some a-axis polarization over an extended range of wave vectors making them observable at momentum transfer along a (Figure 13). Evidently, hybridization and repulsion of the two types of vibrations are quite strong in $YBa_2Cu_3O_{0.7}$.

A P P E N D I X B : A P P E N D I X B : S P E C I A L F O R C E C O N S T A N T S

As mentioned in Section III.1, several special terms have to be added to the shell model to arrive at a quantitative description of the bond-stretching branches. The term describing screening by free carriers has been explained in detail in Ref. 30. The term accounting for a planar breathing deformability has been given in Ref. 30 as well. The parameter A for this planar breathing deformability was tuned to reproduce the observed [14] bond-stretching phonon dispersion in the [110] direction. Although the bond-stretching modes in the [110] direction do show a considerable renormalization with the

metal-insulator transition, the branch remains flat. As a consequence, the parameter A was found to be rather small ($A = 25000$ dyn/cm).

The further terms needed to arrive at a satisfactory description of the bond-stretching branches in the [100] and in the [010] directions are ad hoc extensions of the term for the breathing deformability: a 2×2 sub-matrix is added to the dynamical matrix for the plane oxygen atoms O2 and O3 (and, of course, for the other plane oxygen atoms in the bi-layer as well). The diagonal elements of the matrix are given by

$$D_2(1;1) = B_{100} \sin^2(q_x) + C_{100} \sin^2(2q_x) \sin^2(q_y) \sin^2(q_z)$$

$$D_2(2;2) = B_{010} \sin^2(q_y) + C_{010} \sin^2(2q_y) \sin^2(q_x) \sin^2(q_z)$$

The non-diagonal elements of the matrix are zero. For negative values of B_{100} the frequencies of the bond-

stretching modes are lowered in the [100] direction in a sine-like manner from the zone center to the zone boundary. On the other hand, this term has no effect in both the [010] and in the [110] directions. From a fit to the experimental data we obtained $B_{100} = -70000$ dyn/cm. The parameter C_{100} describes the second harmonic of the linear breathing deformability with a maximum effect at $q = 0.25 a^*$ and zero effect at $q = 0$ and at $q = 0.5 a^*$. The fit resulted in a value $C_{100} = -60000$ dyn/cm. The corresponding terms for the [010] direction were obtained as $B_{010} = -75000$ dyn/cm and $C_{010} = -55000$ dyn/cm.

In order to describe the anomalous softening upon cooling in the [010] direction at least in a semi-quantitative manner another term was added to $D_2(2,2)$ in analogy to the term with the prefactor C_{010} but with the factor $\sin^2(2q_y)$ raised to the n th power. This term was adjusted by trial and error to $C'_{010} = -100000$ dyn/cm and $n = 6$.

-
- [*] Also at Laboratoire Leon Brillouin, CE Saclay, F-91191 Gif-sur-Yvette, France.
- [1] L. Pintschovius and W. Reichardt, in *Neutron Scattering in Layered Copper-Oxide Superconductors*, ed. by A. Furrer, Phys. and Chem. of Materials with Low-D in. Structures, Vol. 20 (Kluwer Academic Publ., Dordrecht, 1998) p. 165.
- [2] L. Pintschovius and M. Braden, Phys. Rev. B 60 R15039 (1999).
- [3] R. J. McQueeney et al., Phys. Rev. Lett. 87 077001 (2001).
- [4] B. Renker et al., Z. Phys. 67 15 (1987); Z. Phys. 71 437 (1988); Z. Phys. 73 309 (1988).
- [5] A. Lanzara et al., Nature 412 510 (2001).
- [6] Z.-X. Shen, A. Lanzara, S. Ishihara, and N. Nagaosa, Philos. Mag. B 82 1349 (2002).
- [7] J. Zaanen and O. Gunnarsson, Phys. Rev. B 40 7391 (1989).
- [8] K. Machida, Physica C 158 192 (1989).
- [9] V. J. Emery, S. A. Kivelson, and H. Q. Lin, Phys. Rev. Lett. 64 4475 (1990).
- [10] A. H. Castro Neto, Phys. Rev. B 64 104509 (2001).
- [11] K. Park and S. Sachdev, Phys. Rev. B 64 184510 (2001).
- [12] E. Kaneshita, M. Ichiohara and K. Machida, Phys. Rev. Lett. 88 115501 (2002).
- [13] B. Renker et al., Phys. Rev. Lett. 30 1144 (1973).
- [14] W. Reichardt, J. Low Temp. Phys. 105, 807 (1996).
- [15] R. J. McQueeney et al., cond-mat/0105593; J.-H. Chung et al., Phys. Rev. B 67, 014517 (2003).
- [16] A brief account of the early results of this study was given in D. Reznik et al., J. Low Temp. Physics 131, 417 (2003). The strong temperature dependence of particular phonons described in Ref. 17 was not yet discovered at the time of this publication.
- [17] L. Pintschovius, Y. Endoh, D. Reznik, H. Hiraka, J. M. Tranquada, W. Reichardt, H. Uchiyama, T. Masui and S. Tajima, cond-mat/0308357.
- [18] S. L. Chaplot, W. Reichardt, L. Pintschovius, and N. Pyka, Phys. Rev. B 52, 7230 (1995).
- [19] N. Pyka, W. Reichardt, L. Pintschovius, S. L. Chaplot, P. Schweiss, A. Erb, and G. Müller-Voigt, Phys. Rev. B 48 7746 (1993).
- [20] We note that there is a systematic difference between the data of ref. 15 and our data of about 1 meV which we attribute to a slightly different calibration of the neutron spectrometers. Our calibration is supported by the good agreement with the optical data of ref. .
- [21] C. Bernhard et al., Solid State Comm. 121 93 (2002).
- [22] We completely agree with Ref. 15 with regard to the a-b anisotropy of the zone-center bond stretching modes. On the other hand, we disagree with Ref. with regard to the anisotropy of the softening at the zone edge: we find that the frequencies are more strongly renormalized in the b direction than in the a direction. We note that the a axis zone boundary mode at $E = 66$ meV was completely ignored in Ref. 8 when evaluating the a-b anisotropy - in spite of the correct observation that this mode carries an appreciable spectral weight. This leads to a substantial overestimate of the renormalization along a.
- [23] K. P. Bohnen, R. Heid and K. Krauss, cond-mat/0211084, to appear in Europhys. Lett.
- [24] O. Rosch and O. Gunnarsson, cond-mat/0308035.
- [25] P. Horsch and G. Khaliullin, to appear in Conference Proceedings 'Highlights in condensed matter physics' (Salerno, May 2003), A. Avello (ed.), American Institute of Physics.
- [26] J. M. Tranquada et al., Nature 375 561 (1995).
- [27] L. Pintschovius et al., Phys. Rev. Lett. 89 037001 (2002).
- [28] We note that the tentative assignment of weak peaks observed in Ref. at energies 70 meV and 61 meV, respectively, to the chain O modes and to c-axis displacements of apical O has to be interchanged.
- [29] K. P. Bohnen, R. Heid and B. Renker, Phys. Rev. Lett. 86 5771 (2001).
- [30] L. Pintschovius et al., Phys. Rev. B 40 2229 (1989).

FIG. 1: Illustration of the effect of the special terms included in the model calculations. Black line: no extra terms. Green line: after inclusion of a (negative) planar breathing deformability chosen such as to reproduce the experimental zone boundary frequency in the (110) direction. Violet line: after inclusion of a special term to lower the frequency of the halfbreathing' mode. Red line: after inclusion of a special term to lower the frequency of the bond-stretching modes halfway to the zone boundary. Blue line: after inclusion of a further term to simulate the anomalous softening at low temperatures. Only the branch with in-plane bond-stretching character is shown for clarity. Note that the special terms directly affect only the vibrations with bond-stretching character. Blue/Red circles denote phonon peak positions at $T = 12\text{K}/200\text{K}$. The blue bar at $q = 0.275$ r.l.u. denotes an ill-defined phonon peak containing also contributions from the next lower phonon branch with bond-bending character.

FIG. 2: Measured (a) and calculated (b) neutron scattering intensity along the a direction from $Q = (4,1,0)$ to $(3.5,1,0)$. This Brillouin zone maximizes the scattering cross section for phonons with strong longitudinal plane oxygen vibrations perpendicular to the chains. Further, it allows one to exploit focusing effects for branches with a downward dispersion. Background, linear in energy and independent of Q , has been subtracted from the experimental raw data to emphasize one-phonon scattering. The calculated one-phonon neutron scattering intensity was corrected for spectrometer resolution.

FIG. 3: The same as Fig.1 but for the b direction. The measurements were carried out from $Q = (1,4,0)$ to $(1,3.5,0)$.

FIG. 4: Colour coded contour plots of the measured and calculated neutron scattering intensities shown in Fig. 1. No data is available for the regions colored in brown. The calculated phonon dispersion curves (without the resolution correction) are shown as blue lines. According to the model, phonon branch anticrossing causes dramatic changes in eigenvectors within the same branches between the zone center and the zone boundary, which results in corresponding changes in one-phonon scattering cross sections. Apart from this effect, there is a 30 % increase of the structure factors of the bond-stretching modes from the zone center to the zone boundary in the $(4,1,0)$ Brillouin zone.

FIG. 5: The same as Fig. 3 but for the b direction. The measurements were carried out from $Q = (1,4,0)$ to $(1,3.5,0)$.

FIG. 6: Calculated dispersion curves of phonon branches of Γ_1 -symmetry and of Γ_1' -symmetry, respectively, as well as experimentally measured phonon peak energies. A row spoint to Agm modes, the other modes being of B_{3u} (B_{2u}) character. Data in the energy range 10 meV – 42 meV were taken from previous measurements on twinned samples[1]. Data for the longitudinal acoustic branches were taken from previous measurements on a small (12 mm^3) detwinned sample[19].

FIG. 7: Neutron spectra taken on a twinned sample at $T = 12 \text{ K}$ with a high resolution configuration. The spectra were fitted with two resp. three Gaussians and a sloping background. The peaks are assigned to branches of Γ_4 -symmetry in the a direction or the b direction, respectively.

FIG. 8: Dispersion of high-energy phonon branches of Γ_4 -symmetry along the a direction as determined on the twinned sample. The full lines were calculated from the model described in the text and the dashed lines were taken from Ref. 23. Note that the ab-initio results[23] were shifted upwards by 1 meV.

FIG. 9: Dispersion of the transverse bond-stretching branches along a^* and along b^* , respectively, as observed on an untwinned sample at $T = 12 \text{ K}$. The high-energy branch and the low energy branch along a^* have in-plane oxygen and chain oxygen character, respectively. Lines are a guide to the eye. The arrows denote the frequencies observed by ellipsometry[21].

FIG. 10: Energy scans taken on a twinned sample at two different temperatures.

FIG. 11: Displacement patterns of the two highest energy zone boundary modes with wave vector $q = (0.5, 0, 0)$ as calculated from two different models A and B. Model A is described in the text and reproduces the anomalously low frequency of the in-plane Cu-O bond-stretching mode by including special terms designed for that effect. This choice leads to a strong hybridization of the in-plane bond-stretching mode and of the c-axis polarized apical O mode with energies of 58 meV and 66 meV, respectively. It corresponds to the situation displayed in Fig. 5. The special terms are omitted in model B which leads to a much higher bond-stretching mode frequency (74 meV) and consequently to a much smaller hybridization with the apical O mode (61 meV).

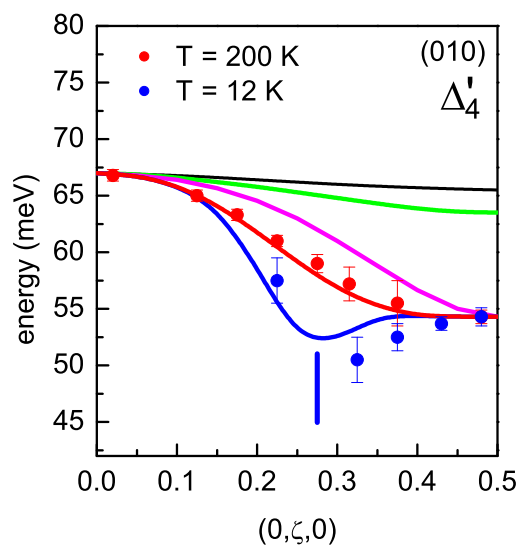
FIG. 12: Colour coded contour plot of calculated 200K neutron scattering intensity for the line from $Q = (1, 4, 0)$ to $(1, 3.5, 0)$. The calculated phonon dispersion curves along the high symmetry line are shown as blue lines. The model used for this plot differs from the one used for Fig. 5 by omitting the special term introduced to describe the anomalous softening observed at low temperatures. The corresponding behavior of the Γ_4' -branches is shown in Fig. 1 by a red line and a blue line, respectively.

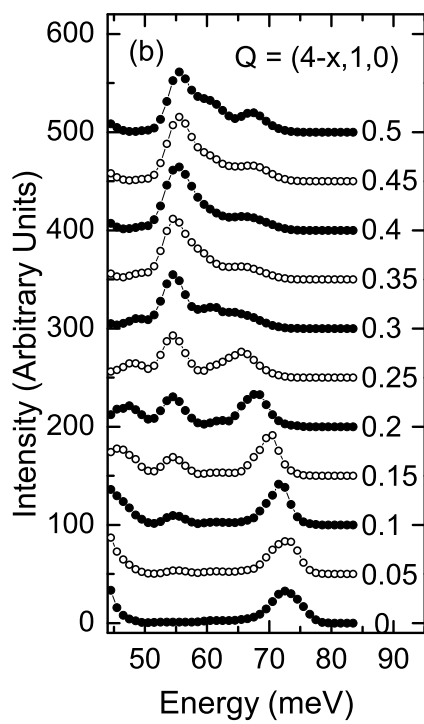
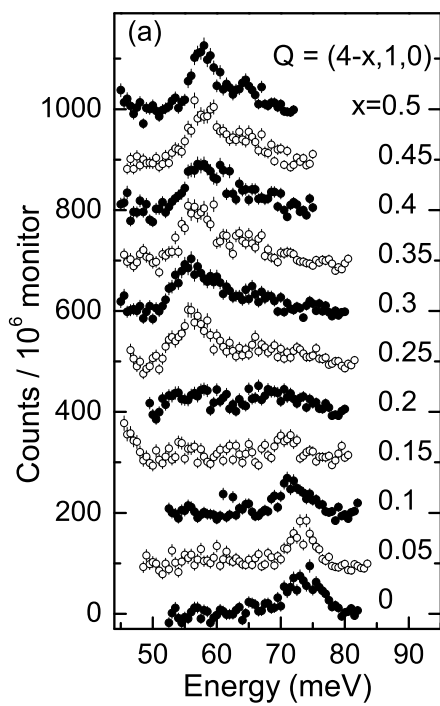
FIG. 13: Top: Calculated dispersion of the two highest Γ_1 -branches before (full lines) and after (dashed lines) inclusion of a special term to reduce the frequencies of the bond-stretching modes half way to the zone boundary. Bottom: inelastic structure factors calculated along the line (3,0,0) to (3.5,0,0).

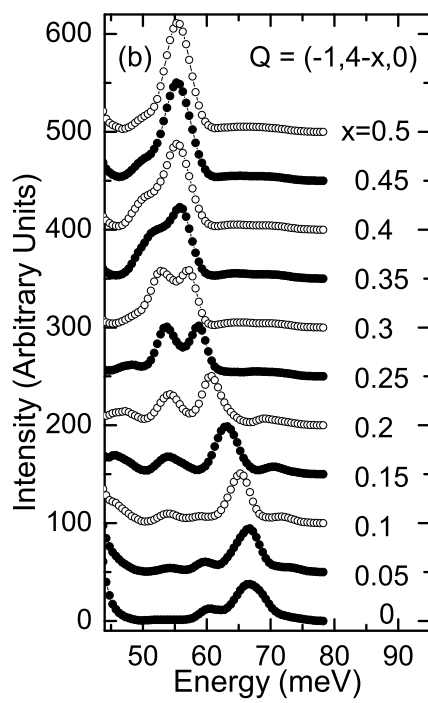
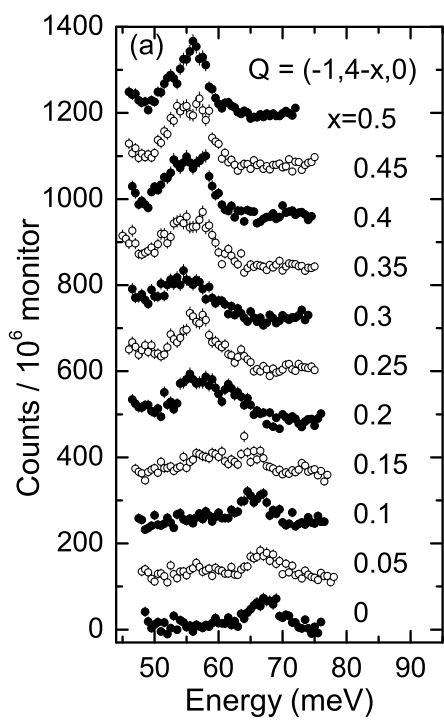
TABLE I: Table I: Parameters of the shell model for $\text{YBa}_2\text{Cu}_3\text{O}_{7-x}$. $Z(k)$, ionic charge; $Y(k)$, shell charge; $K(k)$, core shell force constant. The repulsive Born-Mayer potential used in Ref. 19 was replaced by force constants: F_{kk^0} and G_{kk^0} are longitudinal and transverse force constants, respectively. Following Ref. 19, an attractive van der Waals potential with $C_{kk^0} = 100$ eV Å was assumed to act between oxygen atoms. Note that the chain copper and the chain oxygen are labelled as Cu(1) and O(4), respectively.

k	Z(k)	Y(k)	K(k) (nm ⁻¹)
1= Y	1.85	7.8	8000
2= Ba	1.87	5.6	1200
3= Cu(1)	1.52	2.8	2000
4= Cu(2,3)	1.83	4.2	2000
5= O(1)	-1.62	-2.8	1200
6= O(2,3)	-1.565	-2.2	1200
7= O(4)	-1.26	-2.2	1200

r(Å)	k,k'	F_{kk^0} (dyn/cm)	G_{kk^0} (dyn/cm)
1.859	3,6	375000	-39000
1.9286	4,5	294626	-33892
1.9418	3,7	202706	-21184
1.9611	4,5	264029	-30533
2.2845	4,6	81514	-4615
2.3810	1,5	95669	-13177
2.4075	1,5	95518	-8114
2.6882	6,7	-23182	0
2.7229	5,5	10855	-919
2.7380	2,6	77069	-8662
2.8464	5,5	9734	0
2.8720	2,7	53902	-3158
2.9678	2,5	57065	-8451
2.9890	2,5	44574	-5715
3.1927	5,6	2500	0
3.2090	1,4	0	0
3.2125	5,6	2500	0





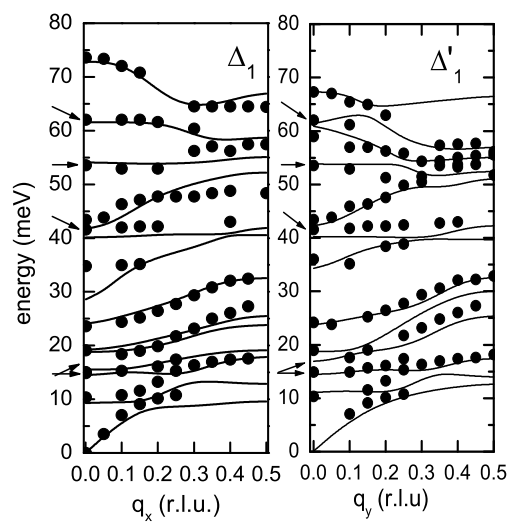


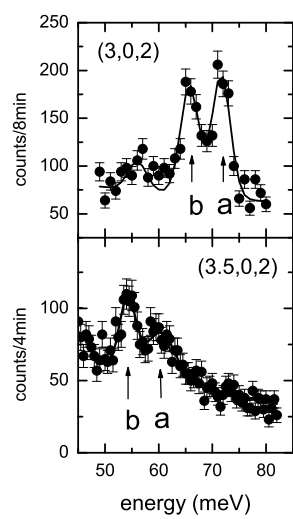
This figure "fig-4.jpg" is available in "jpg" format from:

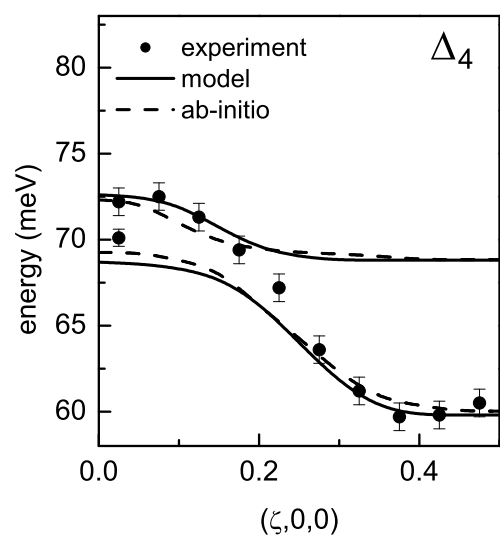
<http://arxiv.org/ps/cond-mat/0310183v1>

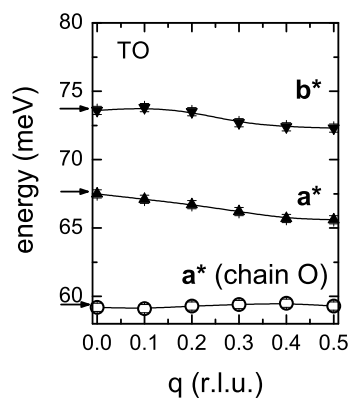
This figure "fig-5.jpg" is available in "jpg" format from:

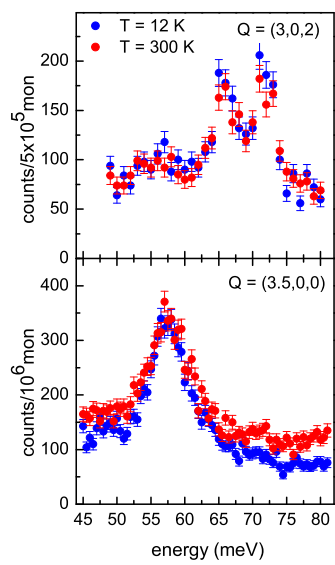
<http://arxiv.org/ps/cond-mat/0310183v1>











This figure "fig-11.jpg" is available in "jpg" format from:

<http://arxiv.org/ps/cond-mat/0310183v1>

